The electric field gradient at the N nuclei and the topology of the charge distribution in the protonation of urea

Yosslen Aray, Carlo Gatti, and Juan Murgich

Citation: The Journal of Chemical Physics **101**, 9800 (1994); doi: 10.1063/1.467945
View online: http://dx.doi.org/10.1063/1.467945
View Table of Contents: http://scitation.aip.org/content/aip/journal/jcp/101/11?ver=pdfcov
Published by the AIP Publishing

The electric field gradient at the N nuclei and the topology of the charge distribution in the protonation of urea

Yosslen Aray
Centro de Química, Instituto Venezolano de Investigaciones Científicas (IVIC), Apartado 21827, Caracas 1020A, Venezuela

Carlo Gatti
Centro CNR per lo Studio delle Relazioni tra Struttura e Reattività Chimica, via Golgi 19, 20133 Milano, Italia

Juan Murgich
Centro de Química, Instituto Venezolano de Investigaciones Científicas (IVIC), Apartado 21827, Caracas 1020A, Venezuela

(Received 8 March 1994; accepted 1 August 1994)

A relationship between some of the critical points of the Laplacian of the charge density of the N valence shell and the electric field gradient (EFG) present at the nucleus of the three-coordinated *N* atom was found for the amine group in urea and some of its adducts and salts. The q_{zz} component of the EFG was shown to be determined by two nonbonded charge distribution local maxima present below and above the molecular plane in the N valence shell. The asymmetry parameter of the EFG was found to be related also to this nonbonded charge concentration. The effect of increasing protonation in urea produced a decrease in the N nonbonded charge concentrations, an increase in bonded concentration along the N–H bond directions and complex fluctuations in the bonded concentration along the N–C bond. The combined effect of the additional H bonds involving the amine group of urea and of the O atom protonation on the N valence shell concentration, is also discussed.

INTRODUCTION

The sensitivity of the electric field gradient at the nucleus to subtle changes in the charge distribution around it has led to an extensive use of this quantity in the study of different electronic effects in molecules and ions in both gaseous and condensed phases.[1,2] In particular, the changes produced by the H bond formation in the charge distribution of acid and base molecules in solids and gases, has been extensively studied.[1,3–5] The electric field gradient (EFG) tensor can be measured by several techniques such as microwave and Mössbauer spectroscopy, nuclear quadrupole, and nuclear magnetic resonance, etc.[2] Generally, the EFGs measured with these techniques have been interpreted in terms of the Mulliken population of localized atomic[2] or molecular orbitals[6] centered at the atom containing the quadrupolar nucleus. Nevertheless, the orbitally based populations are not physical observables as defined by quantum mechanics. It is well known that this type of population analysis is not invariant under unitary transformations. Thus the interpretation of the EFG obtained with one set of orbitals may be not easily related to or even differ from that obtained with another set. Clearly, the information obtained about the charge distribution by means of theories based on arbitrary partitions of subsets of the Hilbert space is open to serious questions based on sound quantum mechanical principles. A more adequate way of obtaining information is the interpretation of the EFG in terms of the electronic charge distribution $\rho(\mathbf{r})$ or quantities directly related to it. One of the main advantages of this approach is that $\rho(\mathbf{r})$ is a physical observable and it is independent of the orbital model used in its calculation. Recently, a way of interpreting the EFG directly in terms of the topology of the Laplacian of the electronic charge distribution $-\nabla^2\rho(\mathbf{r})$ have been developed.[8–10] The study of the $-\nabla^2\rho(\mathbf{r})$ distribution in a free atom shows that the valence shell contains a spherical surface over which $\rho(\mathbf{r})$ is maximally concentrated.[7] The distribution of charge over this surface in the free atom is uniform if one assumes that the nucleus has a negligible electric quadrupole moment. The formation of bonds produces changes in this distribution and a number of local maxima, minima and saddle points appear in the surface of charge distribution which is no longer spherical.[7] A connection between these local extremes of the $-\nabla^2\rho(\mathbf{r})$ of the N valence shell and the EFG present at its nucleus was found for isolated molecules containing one and two coordinated *N* atoms and also in NH_3.[8–10]

Urea forms molecular complexes that exhibit varying degrees of H bonding (or protonation); weak H bonds are present in solid urea[11] and intermediate bonds are found in the urea:oxalic acid 1:1 complex.[12] Stronger H bonds are found, instead, in the urea:phosphoric acid adduct where the acid proton was observed to be midway between the base and the acid molecules at room temperature.[13] In uronium nitrate, in turn, the acidic proton is totally transferred to the base and a covalent O–H bond is formed representing the extreme case of H bonding or protonation.[14,15] A study of the changes in the EFG at the N nucleus resulting from the variation in the degree of protonation will help in the understanding of the subtle effects of the H bond on the charge distribution of the amide group. Once this relationship is obtained, other adducts or salts of urea or similar compounds containing planar amine groups may be studied experimentally and the resulting changes in the charge distribution determined. This is of interest in the study of the fundamental acid–base

 0021-9606/94/101(11)/9800/7/$6.00

interaction and in biochemistry because the amide group forms the backbone of proteins and other biopolymers where the H bonds play an important role in their tertiary structure. Additionally, this study is of interest in the area of nonlinear optical materials where relationships between the hyperpolarizability and the changes introduced in the charge distribution by the H bonds in molecules such as urea have been studied.[16]

In this work, an *ab initio* Hartree–Fock LCAO calculation for crystals and an analysis of the resulting Laplacian topology of the N valence shell of the $-NH_2$ group in urea, the urea:oxalic acid complex and uronium nitrate was performed. In order to evaluate the contribution of the crystal field, calculations for isolated urea, a dimer of urea and of the same adducts studied in the solid state were also done.

COMPUTATIONAL METHODS

The calculation of the *ab initio* SCF wave functions and the critical points of the $-\nabla^2\rho(\mathbf{r})$ in crystalline systems was performed using a modified version[17] of the CRYSTAL 92 program.[18] The choice of basis set is often the most critical step in performing Hartree–Fock calculations of periodic systems. However, no special problems arise in the case of molecular crystals with respect to the isolated molecule case.[18] Tests performed on solid urea and oxalic acid have shown[17] that the 6-21G** basis set is quite adequate and represents a very good compromise, from the point of view of cpu time, of disk space requested, and of the accuracy attainable in the properties of interest. For this reason, in this work, such a basis set was used throughout and, only in pure urea, a 6-31G** set was also employed.

The *ab initio* SCF MO calculations on non periodic systems (isolated molecules, adducts or dimers) were performed (see Fig. 1) using the HONDO-8 (Ref. 19) and GAMESS (Ref. 20) programs with the 6-21G** and 6-31G** basis set.[21] In urea, the molecular geometry (C_{2v} and C_2 symmetry) was optimized with HONDO-8. Since this program and GAMESS use six d functions of the Gaussian-type while CRYSTAL-92 uses only five, single point calculations on isolated molecules were also performed with CRYSTAL-92. Proper comparison of topological properties in gaseous phase and in solid state could be then performed. Also, a calculation of the urea molecule, using the crystal geometry,[22] was performed in order to test the packing effects. In the urea:oxalic acid complex and in the uronium nitrate, the experimental geometry was used in the calculation.[12–15]

For nonperiodic systems, the critical points of the $-\nabla^2\rho(\mathbf{r})$ distribution of the N valence shell were obtained with the BUBBLE program of the new AIMPAC-92 package.[23] The calculations were performed on IBM RISC 6000 Model 530 and 550 workstations.

THEORY

The topological properties of a scalar field such as $\rho(\mathbf{r})$ and its Laplacian $\nabla^2\rho(\mathbf{r})$ are summarized in terms of their critical points $\mathbf{r}_c$, i.e., the points where $\nabla\rho(\mathbf{r})$ and $\nabla[\nabla^2\rho(\mathbf{r})]$ are equal to zero.[7] Critical points are classified according to their type (m,n) by stating their rank m and signature n. The

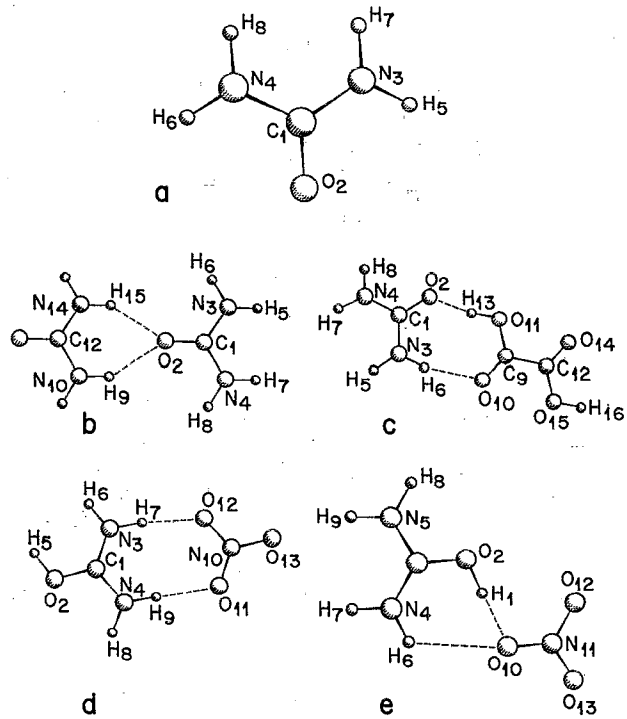

FIG. 1. Molecular arrangement for (a) urea and the different dimers; (b) urea:urea; (c) urea:oxalic acid; (d) uronium nitrate form A; and (e) uronium nitrate form B.

rank is equal to the number of nonzero eigenvalues of the Hessian matrix of $\rho(\mathbf{r})$ [or $\nabla^2\rho(\mathbf{r})$] at $\mathbf{r}_c$ while the signature is the algebraic sum of the signs of the eigenvalues of ρ or $\nabla^2\rho$. The interaction of two atoms leads to the formation of a $(3,-1)$ critical point in the charge distribution and the gradient paths which originate and terminate at this point serve to define, respectively, the bond path and the interaction surface.[7] Only two kinds of critical points in $\rho(\mathbf{r})$ are found in the case of the planar–NH_2 group, the three $(3,-1)$ critical points related to the interaction of N with the two hydrogens and with the rest of the molecule and the $(3,-3)$ critical points found at the position of the nuclei. More complex is, on the other hand, the topology of the Laplacian field, which exhibits another type of critical point; a $(3,+1)$ saddle point in the valence shell of the N atom. This critical point represents a local maximum in one direction and a minimum in the other two. In general, the type and number of critical points in the valence shell of a bonded atom is succinctly summarized by its atomic graph.[7] This graph provides the connectivity of the extremes in the corresponding valence shell distribution and may be seen in Fig. 2 for the N atom present in the amine group in urea.

Of particular interest for the purpose of our work is that the topology of the Laplacian field allows the recovery of the chemical model of the localized bonded and nonbonded pairs and, in general, to characterize local concentrations $[-\nabla^2\rho(\mathbf{r})>0]$ and depletions $[-\nabla^2\rho(\mathbf{r})<0]$ of the electronic distribution. In fact, the Laplacian distribution of $\rho(\mathbf{r})$ for a free atom reflects the quantum shell structure by exhibiting the corresponding number of alternating pairs of shells of

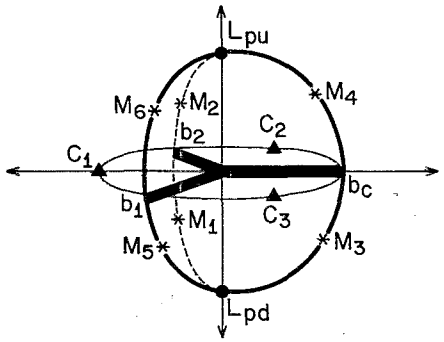

FIG. 2. Atomic graph for the N atom in urea. In this figure, there are (3,−3) critical points in the $-\nabla^2\rho(\mathbf{r})$ distribution along the N–H bond direction (b_1 and b_2), the N–C (b_c) plus two others located above (L_{pu}) and below (L_{pd}) the molecular plane (·). There are also three (3,+1) critical points (C_i, with $i=1$, 2 and 3) in the surface of each of the three resulting faces (▲) plus six (3,−1) critical points (M_i, with $i=1$, 2,...,5, and 6) located (∗) each in the middle of the lines joining the L_p and b_i points. The L_{pu} point corresponds to the highest value of the $-\nabla^2\rho(\mathbf{r})$ distribution at the N valence shell nonbonding concentration.

charge concentration and depletion (the inner shell of each pair always being the region of charge concentration).[7] Upon bonding, local maxima and minima are formed in the valence shell of a bonded atom and their number, type, location and $\nabla^2\rho(\mathbf{r})$ value is a function of the linked atom. The regions where the electronic shells or their extremes are located can not be determined directly from the $\rho(\mathbf{r})$ distribution. This is an obstacle in the analysis of the EFG present at the nucleus directly in terms of $\rho(\mathbf{r})$. Fortunately, the field gradient present at the nucleus reflects predominantly the departure from the spherical symmetry of the atomic shells, so a connection between the extremes found in the $-\nabla^2\rho(\mathbf{r})$ distribution of the valence shell of the quadrupolar atom and the field gradient at its nucleus is anticipated.

The EFG is a traceless, symmetric second rank tensor[2] whose principal axes are chosen such that its components $\mathbf{q}_{ij}=\partial^2 V(\mathbf{r})/\partial\mathbf{x}_i\partial\mathbf{x}_j$ satisfy $|q_{zz}|\geq|q_{yy}|\geq|q_{xx}|$ with $V(\mathbf{r})$ being the external electrostatic potential. Usually, the quadrupole coupling constant, e^2qQ/h (where Q is the nuclear electric quadrupole moment, and $eq=q_{zz}$) plus the asymmetry parameter, $\eta=|(q_{yy}-q_{xx})/q_{zz}|$ are determined experimentally.

BASIS SET AND ELECTRON CORRELATION EFFECTS

The use of finite basis sets and the neglecting of the electron correlation in the MO calculations, introduce uncertainties in the calculated values of the EFG. Recently, it was shown that the 6-31G** basis set was able to reproduce the values of the EFG tensor calculated in HCN and N_2 with sophisticated CI methods due to a cancellation of errors.[24] Similarly, the agreement between the 6-31G** and CI+TZP values for the EFG found for a set of imines and diimides was remarkable (<5%) except for only one component in a particular compound where it was around[10] 15%. These results obtained with the 6-31G** set indicates that its use provides a reasonable compromise between the required accuracy in the EFG components and in the values of $\rho(\mathbf{r})$, the available computer time and disk memory. For the reasons outlined in the computational method section and with the exception of urea, the 6-31G** basis set was employed only in the calculations of the nonperiodical systems. A comparison of the results obtained for the critical point of the $\nabla^2\rho$ of the N valence shell in the isolated dimers with the different basis sets employing the $6d$ and $5d$ functions provides an insight of the importance of its composition. The values of $\nabla^2\rho$ at the different critical points obtained with the 6-21G** set using $5d$ functions and with the same base but with $6d$ showed a linear correlation with R values ranging from 0.998 to 1. A similar correlation was found also for the values obtained with the 6-31G** basis set with 6 and 5 d functions. The values of $\nabla^2\rho$ obtained with a 6-21G** and a 6-31G** set both using $5d$ functions gave a correlation with $R>0.99$. A similar result was found for the $6d$ values obtained with both basis sets. The goodness of the fit encouraged us to extrapolate the values of the $\nabla^2\rho$ obtained with the 6-31G** set in the isolated dimers to the solid state. The values obtained in the solid state with the 6-21G** set were converted by means of the correlation equation determined from the 6-31G** values corresponding to the isolated dimers. These values of $\nabla^2\rho$ were later used in the correlations with the components of the field gradient at the N nucleus.

For the compounds studied here, the trends found for q_{zz} with the 6-31G** ($6d$) set were also well reproduced by the 6-21G** ($6d$) [$q_{zz}(6.21\text{G}^{**})=1.107\ q_{zz}(6\text{-}31\text{G}^{**})+0.134$, $R=0.998$].

The inclusion of the electron correlation can also partially affect the charge density and its associated gradient vector and Laplacian field.[25] However, as showed in imines and di-imides[10] as in some other N containing compounds,[25,26] the quantitative changes in the values of $\rho(\mathbf{r})$ and $-\nabla^2\rho(\mathbf{r})$ at the critical points induced by correlation are relatively small in magnitude. Thus, the values obtained with the 6-31G** or 6-21G** basis set at the Hartree–Fock LCAO level were used in this work.

RESULTS AND DISCUSSION

The topological analysis of the $-\nabla^2\rho(\mathbf{r})$ distribution for the N atoms in the investigated compounds gave atomic graphs of its valence shell topologies equivalent to that found for the planar NH_2 group in isolated urea with the C_{2v} symmetry. The graph showed five (3,−3) critical points (local maxima), one along each of the N–H bond direction b_1 and b_2, one in the N–C bond directions b_c plus two of the nonbonded type L_p. These latter two points are located one above and one below the molecular plane (see Fig. 2). Each L_p point is linked to the b type critical points by three unique trajectories of the $\nabla\nabla^2\rho(\mathbf{r})$. The atomic graph for the $-\nabla^2\rho(\mathbf{r})$ distribution in the N atom in planar amides is, then, a trigonal bypyramid with curved faces as seen in Fig. 2. In the center of each face there is a (3,+1) critical point c_i ($i=1$, 2, and 3) of the $-\nabla^2\rho(\mathbf{r})$ distribution. It is interesting to notice that the value of $-\nabla^2\rho(\mathbf{r})$ at the bonded critical points of the N–H bonds pointing away from the molecule b_2 differs slightly from the other two of the N–H bonds. This

TABLE I. Critical points of the $-\nabla^2\rho(\mathbf{r})$ distribution on the N VSCC in urea, and in some of its adducts and salts.

Molecule, site		b_1 (a.u.)	b_2 (a.u.)	b_c (a.u.)	L_p (a.u.)
Urea cryst.		1.721	1.672	1.657	1.344
geometry		1.997	1.892	1.922	2.271
Urea, C_{2v}		1.766	1.718	1.579	1.358
geometry		2.047	1.952	1.879	2.278
Urea	N10	1.682	1.778	1.644	1.310
dimer		1.933	2.075	1.894	2.202
	N4	1.737	1.700	1.642	1.322
		2.018	1.934	1.888	2.245
Urea	N3	1.886	1.719	1.668	1.297
Oxalic Ac.					1.209
		2.243	1.952	1,874	2.192
					2.070
	N4	1.772	1.730	1.694	1.353
					1.254
		2.061	1.970	1.928	2.285
					2.150
Urea	N3	1.755	2.001	1.704	1.136
nitrate					1.103
		2.017	2.470	1.794	1.969
					1.921
	N4	1.826	1.984	1.670	1.101
					1.017
		2.138	2.437	1.745	1.930
					1.905
Urea	N4	1.869	1.744	1.752	1.214
nitrate					1.175
		2.219	2.017	1.883	2.104
					2.045
	N5	1.850	1.737	1.739	1.235
					1.214
		2.178	2.005	1.887	2.138
					2.107

variation reflects the intrinsic asymmetry that exists in the charge distribution of these bonds in planar amides such as urea. The difference obtained is comparable to that found between the values at b_c and b_1 (or b_2) points and indicates the sensitivity of the $-\nabla^2\rho(\mathbf{r})$ to the asymmetry in the environment of a N atom in such molecules. In Tables I and II are shown the values of the $-\nabla^2\rho(\mathbf{r})$ distribution at the extremes found in the N valence shell of the investigated molecules and complexes. From Tables I and II, one may see the effect of the changes in the geometry of urea on the values of the $-\nabla^2\rho(\mathbf{r})$ at the critical points of the N valence shell. The changes observed in $-\nabla^2\rho(\mathbf{r})$ values were less than 5%; however, the C_2 form of the isolated urea molecule was found to be slightly lower in energy (−1.13 kcal/mol at the 6-31G** level and −1.99 kcal/mol at the MP2/6-31G** level) than the planar C_{2v} geometry. The C_2 form exhibits a N atomic graph with just only one nonbonded maximum "lone pair" in the valence shell. This is the result of the pyramidalization of the planar NH_2 group when the geometry is transformed from C_{2v} to C_2. The changes in the basis sets introduced variations of around 12% to 15% in the values of $-\nabla^2\rho(\mathbf{r})$ at the critical points except for the L_p points where a larger discrepancy was found. Nevertheless, the trends found with a particular basis set were always well reproduced by the others.

TABLE II. Critical points of the $-\nabla^2\rho(\mathbf{r})$ distribution on the N valence shell in solid urea, and some of its solid adducts and salts.

Molecule, site		Basis set	b_1 (a.u.)	b_2 (a.u.)	b_c (a.u.)	L_p (a.u.)
Urea		6-21G**	1.831	1.826	1.587	1.158
		6-31G**	2.181	2.160	1.810	2.022
Urea: oxalic		6-21G*	1.876	1.854	1.635	1.177
acid complex						1.101
Uronium	N3	6-21G*	1.888	1.881	1.697	1.085
Nitrate						1.053
	N4	6-21G*	1.894	1.856	1.689	1.101
						1.082

Generally, the formation of a H bond results in a mutual penetration of the outer nonbonded density of an atom of the base and one of the H atom of the acid.[27] It has been found that there is always a certain degree of charge transfer from the base to the acid molecule. Nevertheless, the transfer is small, in general, when compared to the changes in the individual atomic charges close to the protonation site.[27] This shows that a redistribution of the charge in both the base and the acid molecule occurs upon H bond formation. Such change in the charge distribution will modify the valence shell of each atom in the molecule. The magnitude of the changes will depend on the position of the atom within the molecule and on the degree of protonation achieved. In molecules where a high degree of electronic delocalization exists, it is expected that the effect of protonation will be felt quite a number of bonds away from the coordination site. Such changes may be studied through the variation of the $-\nabla^2\rho(\mathbf{r})$ values at the critical points of the valence shell of atoms forming the molecule. The H bonds connecting the O atom of neighboring urea molecules with the $-NH_2$ group in the crystal introduces perturbations in the critical points at the N valence shell. In general, the more important changes in the N atom will be generated by the intermolecular bonds involving the amine group because, in urea, the protonation site is not directly linked to the N atoms. Then, the changes in the N valence shell produced by the protonation of the O atom in solid urea has to compete with those introduced by the intermolecular H bonds. The final N charge distribution for urea in the solid complexes will, then, reflect the combined effect of both contributions.

Protonation of the O atom in urea does not modify the number, the signature or the rank of its N valence shell critical points. The effect of changes in protonation may be studied by starting first with the study of the isolated urea dimer, proceeding later with the study of a dimer of a stronger complex such as that formed with the oxalic acid and ending with the examination of a dimer of the uronium nitrate, which represents the limiting case of H bonding. This type of study provides information about the effect of the protonation on the charge distribution of the isolated acid–base dimers. In a subsequent step, a similar study of these complexes in the solid state will provide information about other contributions

present in the bulk that modifies the charge distribution of the N atoms.

In the pure urea dimer considered (Fig. 1), there are two sets of N atoms, one (N3 and 4) belonging to the acceptor moiety which undergoes changes in its valence shell due to protonation of the O atom and a second one (N10 and 14), which belongs to the donor moiety, with some of their H atoms directly involved in intermolecular bonds. A comparison of the values of $-\nabla^2\rho(\mathbf{r})$ at the N critical points shows that the formation of the urea dimer produces only small changes in N3 and 4 (b_1 and b_2 increase slightly, while b_c and L_p decrease also slightly). For the N10 and 14, the modifications were more pronounced and the intermolecular bond produces an appreciable increase (9%, at the 6-31G** level) at the b_2 point, while b_1 and L_p are both decreased by 3%, at the same level. For both sets of N atoms, the value of $-\nabla^2\rho$ at the b_c point decreased only slightly ($\approx$1%) upon the dimer formation.

When the critical points of $-\nabla^2\rho(\mathbf{r})$ for the N atoms in a free dimer of the urea:oxalic acid complex are compared with those of isolated urea, one finds that the formation of H bond produces similar effects than in the urea dimer but they are enhanced as the degree of protonation has increased. In this case, N4 (see Fig. 1) turns out to be less perturbed than N3 and the values of the Laplacian at the N–H points of this latter atom, are both increased with respect to isolated urea but by a much different amount (11% and 3%, respectively, at the 6-31G** level). Due to a small departure from planarity of the amine group in this adduct and in the uronium nitrate, as well as in the corresponding solids, the two L_p points of the N valence shell become inequivalent in these complexes. This inequivalence arises from pyrimidalization of the $-NH_2$ group already mentioned. In this configuration, the N valence shell contains only a nonbonded concentration or "lone pair" that occupies one of the four branches of the tetrahedra. Contributions from this form generates an increase in the $-\nabla^2\rho(\mathbf{r})$ value at one of the nonbonded maxima while in the other it is decreased accordingly. As shown in Tables I and II, the formation of the H bond produces a decrease of the values of the Laplacian at the L_p points corresponding to the N atom involved in it. For the other N atoms not involved in the intermolecular bonds, one of their L_p points shows an increase in the value of $-\nabla^2\rho$ while the other exhibits the opposite trend. The decrease in the Laplacian values at the L_p points of the N atom involved in the H bond in the oxalic acid complex is nearly twice of that found in the urea dimer. The changes in $-\nabla^2\rho(\mathbf{r})$ at the b_c point, in this case, are more complex because they are relatively small, depending on the kind of N considered and the type of basis set used as well.

Two different adducts were considered in the limiting case of uronium nitrate; complex A were both N atoms are involved in H bonds and complex B with only the oxydryl H involved in such a bond with a neighboring nitrate ion (see Fig. 1). The first adduct provides information about the combined effect of O–H covalent bond formation and H bonding on the N valence shell of the uronium molecule while the second shows only the effect of O–H covalent bond formation. The values shown in Table I, indicate that both effects make similar contributions to the values of $-\nabla^2\rho(\mathbf{r})$ at the L_p points. The decrease in the Laplacian at L_p points with respect to the uncomplexed urea is 17% for the adduct A and 10% for B at the 6-31G** level. If the values at N4 or 5 in the complex B are compared with those of N4 in the urea dimer and in the urea:oxalic acid complex, a close parallel between the extent of the O protonation and the decrease in the L_p points may be deduced. In the adduct B, the increase in the values of the Laplacian at the b_1 and b_2 points is twice the change found at the N4 in the urea:oxalic acid complex and four times larger than in the urea dimer. In the adduct A, the values at b_1 and b_2 points are much more differentiated than in the N3 atom in the oxalic acid complex and in N10 atom in the urea dimer. The changes obtained for the b_c point for the uronium nitrate again are small but much more complex to analyze than the others as it appears to have a strong dependence with the type of basis set employed in the calculation. Except for N4 in the oxalic acid complex, for the Laplacian at b_c there is an increase with respect to the values found in the isolated urea if one employs the 6-21G** set while an opposite behavior is found if the 6-31G** set is used in the calculation.

A comparison (see Table I) of the results obtained for isolated urea in gaseous phase and its C_{2v} optimized or at its crystal geometry with those obtained in the solid state (Table II) allows an evaluation of the crystal field effects. First, it appears that the changes observed on passing from the gaseous phase to the solid state are mostly due to the presence of the neighboring molecules rather than to changes in geometry. In fact, the changes found when placing an isolated urea molecule in the crystal starting from its C_{2v} optimized or its crystal geometry are qualitatively similar. Moreover, the values of the Laplacian at the L_p points agree even quantitatively, while those at the N–H bonded points are overestimated ($\approx$30%) when the frozen crystal geometry is used for the gaseous phase. The results presented in Tables I and II show that the crystal field strongly enhances the effect of H bond formation on the decrease at the L_p points (14% compared with an average of 2% in the urea dimer, at the 6-21G** level) and the changes in the N–H bonded points. The asymmetry in the N–H bonds is more marked in the urea dimer than in the solid where it is quite small (<1%). In fact, in the solid state, it is no longer possible to isolate a donor or a acceptor moiety (with the resulting enhanced asymmetry of the N–H points) and the overall effect of the H bonds on the N valence shell tends to compensate the intrinsic asymmetry present in the urea molecule. The comparison of the results of the calculation obtained in the solid state shows that the equalization of the values at the N–H points and their noticeable increase (from 6% in solid urea to about 10% in solid uronium nitrate) is a behavior common to all solids studied. The observed decrease in the values of the Laplacian at the L_p points parallels the extent of the O protonation as found in the case of dimers of urea in the gaseous phase. Nevertheless, the values at the L_p points are scattered in a much narrower range in the solid state than in the gas phase. This indicates that the variations generated by the network of H bonds around the amine group in these solids are such that the changes in the N bonded critical points

TABLE III. *Ab initio* EFG components and η values at the N nucleus in urea and some of its adducts and salts.

Molecule, site		Basis set	$-q_{zz}$ (u.a.)	q_{yy} (u.a.)	q_{xx} (u.a.)	η
Urea, experimental geometry		6-21G**	1.075	0.566	0.509	0.053
		6-31G**	1.103	0.574	0.529	0.041
Urea, C_{2v} optimized geometry		6-21g**	1.090	0.569	0.521	0.044
		6-31g**	1.108	0.586	0.523	0.058
Urea dimer	N10	6-21g**	1.021	0.571	0.450	0.118
		6-31g**	1.039	0.596	0.443	0.147
	N4	6-21g**	1.050	0.539	0.511	0.027
		6-31G**	1.084	0.572	0.512	0.055
Urea: oxalic acid dimer	N3	6-21G**	0.951	0.568	0.383	0.190
		6-31G**	0.984	0.609	0.376	0.237
	N4	6-21g**	1.028	0.532	0.496	0.035
		6-31G**	1.062	0.574	0.486	0.082
Uronium nitrate dimer A	N3	6-21G**	0.782	0.585	0.197	0.496
		6-31G**	0.838	0.640	0.197	0.529
	N4	6-21G**	0.767	0.566	0.201	0.475
		6-31G**	0.815	0.621	0.194	0.525
Uronium nitrate dimer B	N4	6-21G**	0.900	0.520	0.380	0.156
		6-31G**	0.953	0.579	0.371	0.215
	N5	6-21G**	0.946	0.524	0.422	0.109
		6-31G**	0.996	0.581	0.415	0.166

seem to be partially compensated by those produced by the protonation of the O atom.

ELECTRIC FIELD GRADIENT AND THE LAPLACIAN OF ρ

In Table III are shown the principal values of the EFG tensor obtained in this work. In general, the values obtained for both geometries and basis sets were quite close and only small variations were found for the EFG components of the isolated urea molecule. In the dimer of urea, there is a significant difference between the N involved in the H bonds N10 and the uncomplexed one N4. A similar behavior was also found for their $-\nabla^2\rho(\mathbf{r})$ distribution. The N4 atom shows values of the EFG components close to those of the isolated urea while in the N10 atom, a decrease in the q_{zz} and an important increase in the η value was observed as found experimentally in protonated urea.[4,5]

The relationship of the N EFG with the topology of $\rho(\mathbf{r})$ may be explored by relating its components and the directions of its principal axes with the extremes of the $-\nabla^2\rho(\mathbf{r})$ distribution of the N valence shell and their position within the atomic graph. As mentioned above, the main contribution to the EFG originates in the asymmetries of the N valence shell distribution which are reflected in its Laplacian critical points. Even if the neighboring atoms do contribute to the EFG,[8,10] as one is interested in determining the general trends produced by the protonation in urea, only the main contribution arising from the N valence shell will be analyzed here. In Tables I and II are shown the values of the $-\nabla^2\rho(\mathbf{r})$ in different critical points of the valence shell of the N atom in free and protonated urea both in the gaseous and solid state. An inspection of the N atomic graph of Fig. 2 and the results shown in Tables I and II indicate that one of the directions in which the electronic distribution changes most noticeably is along the direction of the two nonbonded charge concentrations found in the N valence shell. This direction corresponds to that of the principal z axis of the EFG as found experimentally[2] and in this calculation for the planar $-NH_2$ group. The direction of the N–C bond coincides with the principal y axis of the EFG showing that its orientation is related to the critical points of the $-\nabla^2\rho(\mathbf{r})$ distribution. A correlation between q_{zz} and the $-\nabla^2\rho(\mathbf{r})$ values at the L_p points obtained with the 6-21G** basis set showed a good fit with $R=0.981$. In this correlation, both the isolated dimers and the solid state $-\nabla^2\rho(\mathbf{r})$ values at the L_p points were considered. The values of q_{zz} for crystalline urea and the solid complexes were those obtained experimentally while for the isolated dimers and molecule, only the calculated values of q_{zz} were employed. A similar correlation ($q_{zz}=0.794\ L_p-0.724$) but using extrapolated 6-31G** values for the crystals from the correlation with the 6-21G** results, gave a value of $R=0.970$. A multilinear correlation ($q_{zz}=0.437\ L_{pu}+0.449\ L_{pl}+0.007\ b_c-0.001\ b_1+0.049\ b_2$, $R=1.000$) showed that the main contribution to q_{zz} (94%) arises from the nonbonded charge concentrations (L_{pu} and L_{pl}) located at both upper and lower L_p points (see Fig. 2). The contribution to q_{zz} from the extremes at the N–H and N–C bond directions is an order of magnitude smaller (6%). This shows that the nonbonded concentrations of the N valence shell at the L_p points determine the principal component q_{zz} of the N EFG in planar amines.

The asymmetry parameter η showed a good correlation ($\eta=-1.329\ L_{pu}+3.092$, $R=0.972$ and $\eta=-1.273\ L_{pl}+2.915$, $R=0.970$) with the $-\nabla^2\rho(\mathbf{r})$ values at the L_p points. Nevertheless, the dependence with the values of the $-\nabla^2\rho(\mathbf{r})$ was just the opposite to that found for q_{zz}. It was found that an increase in the Laplacian at L_p produces a decrease in the N quadrupole coupling constant but an increase in the asymmetry parameter. This result explains the relationship observed between the measured coupling constants and asymmetry parameters for the urea complexes.[8,4] If a multilinear correlation between the values of the Laplacian at both L_p points is considered, one finds ($\eta=-0.651\ L_{pl}-0.704\ L_{pu}+3.118$, $R=0.991$) so their contribution to η is almost the same. As the value of $-\nabla^2\rho(\mathbf{r})$ decreases at the L_p points with protonation, there is an increase in the charge transfer from these points toward the xz molecular plane. Then, this process increases the asymmetry in the charge distribution around the N nucleus that is reflected in the resulting asymmetry parameter. The value of η is expected to have some contributions from the values of the bonded maxima in the directions of the N–C and N–H bonds. Nevertheless, a multilinear correlation involving the values of $-\nabla^2\rho(\mathbf{r})$ showed that their contribution to the asymmetry parameter was negligible.

CONCLUSIONS

The protonation of the O atom in urea produces complex changes in the valence shell of the N atoms that has to be

added to those introduced by the H bonds of the amine group in the solid state. As the degree of protonation increases, the two nonbonded charge concentrations found in the N valence shell decrease, the bonded maxima located along the N–H bond directions increase, and the remaining one placed along the N–C direction show complex fluctuations. The main component of the EFG q_{zz} present at the N nucleus was found to be determined mainly by the two nonbonded charge concentrations located below and above the molecular plane at L_p critical points while the asymmetry parameter was found to be correlated with the value of $\nabla^2\rho(\mathbf{r})$ at the same point.

A multilinear correlation was found also between the values of the $-\nabla^2\rho(\mathbf{r})$ found at the L_p points and at the bonded maximum in the N–H bond direction with the asymmetry parameter. The above result shows that the use of the $\nabla^2\rho(\mathbf{r})$ distribution allows the interpretation of the EFG directly in terms of topology of an observable such as $\rho(\mathbf{r})$ without the use of quantities of doubtful physical meaning.

ACKNOWLEDGMENTS

This work has been done within a joint research project sponsored jointly by the CONICIT of Venezuela and the CNR of Italy. Y.A. and C.G. wants to thank the kind hospitality provided, respectively, by the CSRSRC of the CNR, Milano and IVIC, Caracas; Y.A. and J.M. want also to acknowledge the contribution of the Centro Científico of IBM de Venezuela S.A. and of INTEVEP S.A., Centro de Investigación y Desarrollo de Petróleos de Venezuela, for providing an IBM-RISC 6000 Model 530 workstation.

[1] J. A. S. Smith, Chem. Soc. Rev. **15**, 225 (1986).
[2] E. A. C. Lucken, *Nuclear Quadrupole Coupling Constants* (Academic, New York, 1969).
[3] R. A. Marino, J. Murgich, M. Gourdji, A. Péneau, and L. Guibé, New J. Chem. **11**, 495 (1987).
[4] J. Murgich and M. Santana R., J. Chem. Phys. **74**, 3788 (1981).
[5] H. Negita, T. Kubo, and H. Kato, Bull. Chem. Soc. Jpn. **54**, 391 (1981).
[6] F. A. Cotton and C. B. Harris, Proc. Natl. Acad. Sci. **56**, 12 (1966).
[7] R. F. W. Bader, *Atoms in Molecules: A Quantum Theory* (Clarendon, Oxford, 1990).
[8] Y. Aray and J. Murgich, J. Chem. Phys. **91**, 293 (1989).
[9] Y. Aray, J. Murgich, and M. Luna, J. Am. Chem. Soc. **113**, 7135 (1991).
[10] Y. Aray and J. Murgich, J. Chem. Phys. **97**, 9154 (1992).
[11] R. F. Stewart, NATO ASI Series B, Phys. **250**, 63 (1993).
[12] S. Harkema, J. H. M. Brake, and R. B. Helmholdt, Acta Crystallogr. C **40**, 1733 (1984).
[13] D. Mootz and K. R. Albrand, Acta Crystallogr. B **28**, 2459 (1972).
[14] J. E. Worsham and W. R. Busing, Acta Crystallogr. B **25**, 572 (1969).
[15] S. Harkema and D. Feil, Acta Crystallogr. B **25**, 589 (1969).
[16] J. Zyss and G. Berthier, J. Chem. Phys. **77**, 3635 (1982).
[17] C. Gatti and V. R. Saunders (private communication, 1993).
[18] R. Dovesi, V. R. Saunders, and C. Roetti, Theoretical Chemistry Group, University of Turin, Italy and SERC, Daresbury Laboratory, United Kingdom, 1992.
[19] IBM Corporation Center for Scientific and Engineering Computation, Kingston, New York, 1990.
[20] M. W. Schmidt, J. A. Boatz, K. K. Baldridge, S. Koseki, M. Gordon, S. T. Elbert, and B. Low, QCPE **7**, 115 (1987) and (1990).
[21] R. Ditchfield, W. J. Hehre, and J. A. Pople, Chem. Phys. **54**, 724 (1970).
[22] A. W. Pryor and P. L. Sanger, Acta Crystallogr. A **26**, 543 (1970).
[23] R. F. W. Bader (private communication, 1992).
[24] D. Cremer and M. Krüger, J. Phys. Chem. **96**, 3239 (1992).
[25] C. Gatti, P. J. MacDougall, and R. F. W. Bader, J. Chem. Phys. **88**, 3792 (1988).
[26] R. J. Boyd and L. C. Wang, J. Comp. Chem. **10**, 367 (1989).
[27] M. T. Carroll and R. F. W. Bader, Mol. Phys. **65**, 695 (1988).